# Soliton formation by decelerating interacting Airy beams

**Falko Diebel,[1,*] Bojana M. Bokić,[2] Dejan V. Timotijević,[2] Dragana M. Jović Savić,[2] and Cornelia Denz[1]**

[1]*Institut für Angewandte Physik and Center for Nonlinear Science (CeNoS), Westfälische Wilhelms-Universität Münster, 48149 Münster, Germany*
[2]*Institute of Physics, University of Belgrade , P.O. Box 68, 11080 Belgrade, Serbia*
[*]*falko.diebel@uni-muenster.de*

**Abstract:** We demonstrate a new type of soliton formation arising from the interaction of multiple two-dimensional Airy beams in a nonlinear medium. While in linear regime, interference effects of two or four spatially displaced Airy beams lead to accelerated intensity structures that can be used for optical induction of novel light guiding refractive index structures, the nonlinear cross-interaction between the Airy beams decelerates their bending and enables the formation of straight propagating solitary states. Our experimental results represent an intriguing combination of two fundamental effects, accelerated optical beams and nonlinearity, together enable novel mechanisms of soliton formation that will find applications in all-optical light localization and switching architectures. Our experimental results are supported by corresponding numerical simulations.



**OCIS codes:** (190.4420) Nonlinear optics, transverse effects in; (190.6135) Spatial solitons; (350.5500) Propagation; (190.5330) Photorefractive optics; (140.3300) Laser beam shaping; (070.6120) Spatial light modulators

## References and links

1. M. V. Berry and N. L. Balazs, "Nonspreading wave packets," Am. J. Phys. **47**, 264 (1979).
2. G. A. Siviloglou and D. N. Christodoulides, "Accelerating finite energy Airy beams," Opt. Lett. **32**, 979–981 (2007).
3. G. A. Siviloglou, J. Broky, A. Dogariu, and D. N. Christodoulides, "Observation of Accelerating Airy Beams," Phys. Rev. Lett. **99**, 213901 (2007).
4. J. Broky, G. A. Siviloglou, A. Dogariu, and D. N. Christodoulides, "Self-healing properties of optical Airy beams," Opt. Express **16**, 12880–12891 (2008).
5. J. Baumgartl, M. Mazilu, and K. Dholakia, "Optically mediated particle clearing using Airy wavepackets," Nat. Photonics **2**, 675–678 (2008).
6. M. A. Bandres, I. Kaminer, M. Mills, B. Rodríguez-Lara, E. Greenfield, M. Segev, and D. N. Christodoulides, "Accelerating Optical Beams," Opt. Photonics News **24**, 30–37 (2013).
7. A. Mathis, F. Courvoisier, L. Froehly, L. Furfaro, M. Jacquot, P. A. Lacourt, and J. M. Dudley, "Micromachining along a curve: Femtosecond laser micromachining of curved profiles in diamond and silicon using accelerating beams," Appl. Phys. Lett. **101**, 071110 (2012).
8. P. Polynkin, M. Kolesik, J. V. Moloney, G. A. Siviloglou, and D. N. Christodoulides, "Curved Plasma Channel Generation Using Ultraintense Airy Beams," Science **324**, 229–232 (2009).
9. A. Chong, W. H. Renninger, D. N. Christodoulides, and F. W. Wise, "Airy-Bessel wave packets as versatile linear light bullets," Nat. Photonics **4**, 103–106 (2010).
10. N. K. Efremidis, "Airy trajectory engineering in dynamic linear index potentials," Opt. Lett. **36**, 3006–3008 (2011).
11. N. K. Efremidis, "Accelerating beam propagation in refractive-index potentials," Phys. Rev. A **89**, 023841 (2014).

#246589 Received 23 Jul 2015; accepted 28 Jul 2015; published 8 Sep 2015

12. K. G. Makris, I. Kaminer, R. El-Ganainy, N. K. Efremidis, Z. Chen, M. Segev, and D. N. Christodoulides, "Accelerating diffraction-free beams in photonic lattices," Opt. Lett. **39**, 2129–2132 (2014).
13. S. Chávez-Cerda, U. Ruiz, V. Arrizón, and H. M. Moya-Cessa, "Generation of Airy solitary-like wave beams by acceleration control in inhomogeneous media," Opt. Express **19**, 16448–16454 (2011).
14. N. M. Lučić, B. M. Bokić, D. Z. Grujić, D. V. Pantelić, B. M. Jelenković, A. Piper, D. M. Jović, and D. V. Timotijević, "Defect-guided Airy beams in optically induced waveguide arrays," Phys. Rev. A **88**, 063815 (2013).
15. F. Diebel, B. M. Bokić, M. Boguslawski, A. Piper, D. V. Timotijević, D. M. Jović, and C. Denz, "Control of Airy-beam self-acceleration by photonic lattices," Phys. Rev. A **90**, 033802 (2014).
16. P. Rose, F. Diebel, M. Boguslawski, and C. Denz, "Airy beam induced optical routing," Appl. Phys. Lett. **102**, 101101 (2013).
17. R. Bekenstein and M. Segev, "Self-accelerating optical beams in highly nonlocal nonlinear media," Opt. Express **19**, 23706–23715 (2011).
18. Y. Hu, S. Huang, P. Zhang, C. Lou, J. Xu, and Z. Chen, "Persistence and breakdown of Airy beams driven by an initial nonlinearity," Opt. Lett. **35**, 3952–3954 (2010).
19. Y. Hu, G. A. Siviloglou, P. Zhang, N. K. Efremidis, D. N. Christodoulides, and Z. Chen, *Nonlinear Photonics and Novel Optical Phenomena*, vol. 170 of *Springer Series in Optical Sciences* (Springer New York, New York, NY, 2012).
20. R. Driben, V. V. Konotop, and T. Meier, "Coupled Airy breathers," Opt. Lett. **39**, 5523–5526 (2014).
21. Y. S. Kivshar and G. P. Agrawal, *Optical Solitons: From Fibers to Photonic Crystals* (Academic Press, San Diego, 2003).
22. C. Denz, M. Schwab, and C. Weilnau, *Transverse-Pattern Formation in Photorefractive Optics*, vol. 188 of *Springer Tracts in Modern Physics* (Springer, Berlin, 2003).
23. F. Lederer, G. I. Stegeman, D. N. Christodoulides, G. Assanto, M. Segev, and Y. Silberberg, "Discrete solitons in optics," Phys. Rep. **463**, 1–126 (2008).
24. B. Terhalle, T. Richter, A. S. Desyatnikov, D. N. Neshev, W. Królikowski, F. Kaiser, C. Denz, and Y. S. Kivshar, "Observation of Multivortex Solitons in Photonic Lattices," Phys. Rev. Lett. **101**, 013903 (2008).
25. F. Diebel, D. Leykam, M. Boguslawski, P. Rose, C. Denz, and A. S. Desyatnikov, "All-optical switching in optically induced nonlinear waveguide couplers," Appl. Phys. Lett. **104**, 261111 (2014).
26. Y. Zhang, M. R. Belić, Z. Wu, H. Zheng, K. Lu, Y. Li, and Y. Zhang, "Soliton pair generation in the interactions of Airy and nonlinear accelerating beams," Opt. Lett. **38**, 4585–4588 (2013).
27. Y. Zhang, M. R. Belić, H. Zheng, H. Chen, C. Li, Y. Li, and Y. Zhang, "Interactions of Airy beams, nonlinear accelerating beams, and induced solitons in Kerr and saturable nonlinear media," Opt. Express **22**, 7160–7171 (2014).
28. I. M. Allayarov and E. N. Tsoy, "Dynamics of Airy beams in nonlinear media," Phys. Rev. A **90**, 023852 (2014).
29. A. A. Zozulya and D. Z. Anderson, "Propagation of an optical beam in a photorefractive medium in the presence of a photogalvanic nonlinearity or an externally applied electric field," Phys. Rev. A **51**, 1520 (1995).
30. J. A. Davis, D. M. Cottrell, J. Campos, M. J. Yzuel, and I. Moreno, "Encoding Amplitude Information onto Phase-Only Filters," Appl. Opt. **38**, 5004–5013 (1999).
31. U. B. Dörfler, R. Piechatzek, T. Woike, M. K. Imlau, V. Wirth, L. Bohatý, T. Volk, R. Pankrath, and M. Wöhlecke, "A holographic method for the determination of all linear electrooptic coefficients applied to Ce-doped strontium-barium-niobate," Appl. Phys. B Lasers Opt. **68**, 843–848 (1999).
32. N. K. Efremidis and D. N. Christodoulides, "Abruptly autofocusing waves," Opt. Lett. **35**, 4045–4047 (2010).
33. D. G. Papazoglou, N. K. Efremidis, D. N. Christodoulides, and S. Tzortzakis, "Observation of abruptly autofo-cusing waves," Opt. Lett. **36**, 1842–1844 (2011).
34. W. Królikowski, C. Denz, A. Stepken, M. Saffman, and B. Luther-Davies, "Interaction of spatial photorefractive solitons," Quantum Semiclassical Opt. J. Eur. Opt. Soc. Part B **10**, 823 (1998).

## 1. Introduction and motivation

Airy wave packets, first predicted by Berry and Balazs [1] as free-particle solutions of the Schrödinger equation are remarkable objects within the framework of quantum mechanics. The envelope of these wave packets is described by Airy functions, centered around a parabolic trajectory. Their unique ability to freely accelerate during propagation – even in the absence of any external potential – stands out the Airy wave from any other known solution. Airy wave packets were also predicted [2], and then realized [3] in the optical domain. Their special self-healing properties – self-restoration of their canonical form after passing small obstacles – were demonstrated theoretically and experimentally [4]. The unique ballistic-like and self-accelerating properties of the Airy beam made it ideally suited for various applications ranging from particle and cell micromanipulation, optical snow-blowers [5,6], laser micromachining [7]

#246589 Received 23 Jul 2015; accepted 28 Jul 2015; published 8 Sep 2015

and self-bending plasma channels [8] to ultrafast self-accelerating pulses [9].

While the potential of tailored light fields, especially Airy beams, is well recognized in these fields, they are also of significant importance for advances in discrete and nonlinear modern photonics. On the one hand, the influence of inhomogeneous refractive index potentials on Airy beams has been investigated theoretically to design the beam caustics [10–12], on the other hand it was experimentally demonstrated that a linear refractive index gradient or a photonic lattice can be used to control and compensate the Airy beam self-acceleration [13–15]. Another inventive idea shifts the perspective and uses two-dimensional Airy beams itself to optically induce light guiding structures for optical routing and switching of signals [16].

By considering nonlinearity a new degree of freedom is added to the system which leads to interesting new effects of Airy beam propagation investigated in several theoretical and experimental studies [17–20]. One of the most fundamental effect in nonlinear systems is the existence of spatial solitons which represents localized structures that always preserve their shape by the balance between diffraction and nonlinear self-focusing. In optics, they have extensively been studies in various systems, including bulk nonlinear media or discrete systems [21–23], where fundamental solitons or even vortex solitons [24, 25] have been found. The interesting question now is if solitons or solitary structures can arise from the interaction of initially accelerated beams such as Airy beams. Very recently, first numerical studies have started to explore the interaction between two one-dimensional Airy beams in an isotropic idealized nonlinear model [26–28].

In this paper, we investigate the nonlinear interaction of two-dimensional Airy beams experimentally, as well as numerically. Therefore, we introduce advanced experimental methods to synthesize multiple accelerated Airy beams with fully controllable parameters and observe the nonlinear dynamics of this compound optical field in a photorefractive nonlinear crystal, an ideal experimental testbed for nonlinear light-matter interaction. We demonstrate that these interactions lead to solitary structures that arise from nonlinear interaction of two or four involved accelerated Airy beams. Depending on the beam intensity and on different phase configurations of the synthesized beams (in phase or out of phase), either one solitary solution or a pair is observed that propagates almost stable with small intensity modulations (breathing). Moreover, we demonstrate how the synthesized beams propagate in the linear regime, where interference leads to interesting intensity modulations, including tight-focus structures. To precisely describe all our experimental observations in a theoretical framework, we extend and generalize existing concepts to handle multiple Airy beams, as well as nonlinear propagation in the more realistic anisotropic photorefractive model.

## 2. Theoretical model and numerical methods

To study the propagation characteristics of Airy beams in a nonlinear optical system with intensity dependent refractive index modulations, we consider the scaled paraxial equation of diffraction for the envelope $A$ of the optical field:

$$\mathrm{i}\frac{\partial A}{\partial \zeta}+\frac{1}{2}\left(\frac{\partial^2 A}{\partial \chi^2}+\frac{\partial^2 A}{\partial \nu^2}\right)+\frac{1}{2}k_0^2 w_0^2 \Delta n^2(I)A=0. \tag{1}$$

Here, $\chi = x/\mathrm{w}_0$ and $\nu = y/\mathrm{w}_0$ are the dimensionless transverse coordinates scaled by the characteristic length $\mathrm{w}_0$. $\zeta = z/k\mathrm{w}_0^2$ represents the dimensionless propagation distance with $k = 2\pi n/\lambda$.

In this equation, the nonlinearity is given by an intensity-dependent refractive index modulation $\Delta n^2(I)$, with $I \propto |A|^2$, which is caused by the nonlinear response of a photorefractive medium. Theoretically, it is well described by the electro-optic effect combined with the band transport model, which in our case can be approximated by the full anisotropic model for the

#246589 Received 23 Jul 2015; accepted 28 Jul 2015; published 8 Sep 2015

optically induced space charge potential $\phi$, [29]

$$\nabla^2\phi + \nabla\ln(1+I)\cdot\nabla\phi = E_{\text{ext}}\frac{\partial}{\partial x}\ln(1+I) + \frac{k_{\text{B}}T}{e}\left(\nabla^2\ln(1+I) + (\nabla\ln(1+I))^2\right), \quad (2)$$

where the refractive index modulation results from the electro-optic effect as $\Delta n^2 = n_0^4 r_{\text{eff}}\partial_x\phi$, and $r_{\text{reff}}$ is the effective electro-optic coefficient.

This model precisely describes the optical induction process in a photorefractive nonlinear medium with applied electric field $E_{\text{ext}}$ along the crystal's c-axis and accounts for the orientation anisotropy caused by the resulting directed transport of charge carriers. Moreover, this model is capable to describe the effect of charge carrier diffusion in the internal space charge field. This effects plays an important role for non-zero temperatures $T$ and non-zero dark conductivity of the crystal, and leads to effects such as nonlinear soliton steering in bulk nonlinear media.

### *2.1. Two-dimensional Airy beams*

In the linear regime, where $\Delta n(I) = 0$ holds, the wave equation can be solved by two-dimensional truncated Airy beam solutions that reads as

$$\psi(\chi,\nu,\zeta) = A_0\varphi(\chi,\zeta)\varphi(\nu,\zeta), \quad (3)$$

with

$$\varphi(X,\zeta) = \text{Ai}\left[X - \frac{\zeta^2}{4} + \text{i}a_X\zeta\right] \exp\left[\frac{\text{i}}{12}\left(6a_X^2\zeta - 12\text{i}a_X X + 6\text{i}a_X\zeta^2 + 6X\zeta - \zeta^3\right)\right], \text{ with } X = \{\chi,\nu\} \quad (4)$$

Here, $\text{Ai}(X)$ is the Airy function, $A_0$ the amplitude and $a_X$ a positive decay length that truncates the solution to become physically relevant. In the focal plane ($\zeta = 0$) the one-dimensional Airy functions reads as $\varphi(X,0) = \text{Ai}[X]\exp[a_X X]$, where the exponential decay clearly can be seen. Without this truncations the solution will extended over the whole space and contains infinite energy. These truncated solutions still solves the wave equation (1) and the distinguished properties of Airy beams are mostly preserved [2]

### *2.2. Numerical methods*

Due to the inhomogeneous refractive index modulation $\Delta n^2(I_{\text{indu}})$, which here is caused by the nonlocal, anisotropic photorefractive nonlinearity, the paraxial wave equation (1) cannot be solved analytically. Thus, we have implemented comprehensive numerical methods to solve this equation and model the light propagation in nonlinear media. The propagation equation (1) is evaluated numerically, using split-step Fourier methods. In the nonlinear regime, the inducing intensity $I_{\text{indu}} = |A|^2$ is given by the intensity of the propagating wave field itself (cf. equation (1)). Therefore, it is crucial to calculate the optically induced refractive index modulation for each propagation step. This index modulation, represented by $\Delta n^2(I_{\text{indu}})$, is calculated in full anisotropic model [29] using a relaxation method.

## 3. Experimental realization of interacting Airy beams in photorefractive media

All the experiments presented here are performed using the setup sketched in Fig. 1(a). The light from a frequency-doubled Nd:$YVO_4$ laser continuously emitting light at a wavelength of $\lambda = 532\,\text{nm}$ is expanded and illuminates a programmable, high-resolution phase-only spatial light modulator (SLM). The plane wave that enters the modulator experiences a spatial phase

#246589 Received 23 Jul 2015; accepted 28 Jul 2015; published 8 Sep 2015

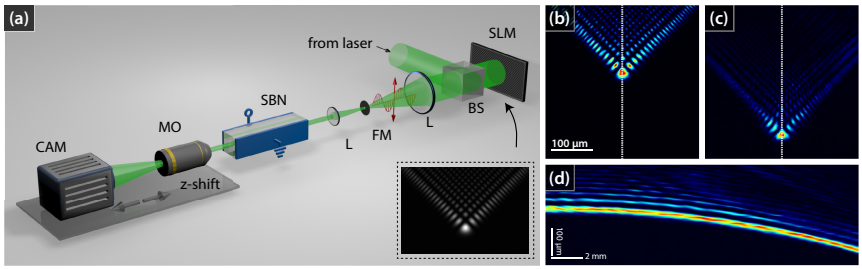


Fig. 1. Experimental setup and single Airy beam characteristics. (a) Experimental setup (SLM: Spatial light modulator, BS: beam splitter, FM: Fourier mask, SBN: strontium barium niobate crystal, MO: microscope objective). (b–d) Linear propagation of a single two-dimensional Airy beam through the homogeneous crystal. (b),(d): Intensity at the input and output face of the crystal, (c) cross-section during propagation.

modulation, which in combination with two following lenses and a Fourier filter leads to any desired complex light field at the input face of the nonlinear photorefractive medium. Therefore, we address an explicitly designed phase pattern to the SLM that allows us to modulate phase and amplitude of the light field at the same time [30]. In this way, we realize different complex light fields as combination of multiple displaced two-dimensional Airy beams, whose field distributions are calculated with equation (3).

This structured beam then illuminates the 20 mm long photorefractive $Sr_{0.60}Ba_{0.40}Nb_2O_6$ (SBN:Ce) crystal which is externally biased with an electric dc field of $E_{\text{ext}} \approx 1000\,\text{V}\,\text{cm}^{-1}$ aligned along the optical c-axis. We take care that the input face of the crystals coincides with the plan corresponding to the SLM's surface. To maximize the nonlinear self-action of the written refractive index structure onto the beam itself – in other words the nonlinearity – the beam is set to be extraordinarily polarized with respect to the crystal's optical c-axis. The high electro-optic coefficient of SBN:Ce [31] facilitates sufficient nonlinearity to substantially change the propagation of the Airy beam. By illuminating the crystal homogeneously with white light, we can erase written refractive index modulations. This reversibility make our experimental approach highly flexible to perform series of experiments using the same nonlinear material. By means of an microscope objective and a camera mounted on a translation stage we can record the intensity distribution in different transverse planes.

## 4. Linear propagation of multiple Airy beams

The propagation characteristics of single Airy beams have been subject to many experimental and numerical studies in the past years, considering linear and nonlinear effects, or propagation in inhomogeneous or periodically structured media. As it is well known, for linear propagation in a homogeneous environment the Airy beams follows a parabolic trajectory while propagation. This behavior can clearly be seen from the experimentally recorded intensity profile of one single Airy beam (Figs. 1(b)–1(d)) realized with the presented experimental setup (Fig. 1(a)). Although the main scope of this work is the interaction of multiple Airy beams, these basic result are presented to demonstrate that our experimental approach and setup allow to realize two-dimensional accelerated Airy beams with very high accuracy. These results serve as a good starting point for the following experimenters about multiple interacting Airy beams.

To systematically investigate the propagation and interaction of multiple two-dimensional Airy beams, we start our studies with considering the most fundamental case of two co-propagating Airy beams in the linear regime. The beams are coherently superimposed with an initial distance of $d \approx 50\,\mu\text{m}$ and are rotated by 180°, so that their accelerated trajectories

#246589 Received 23 Jul 2015; accepted 28 Jul 2015; published 8 Sep 2015

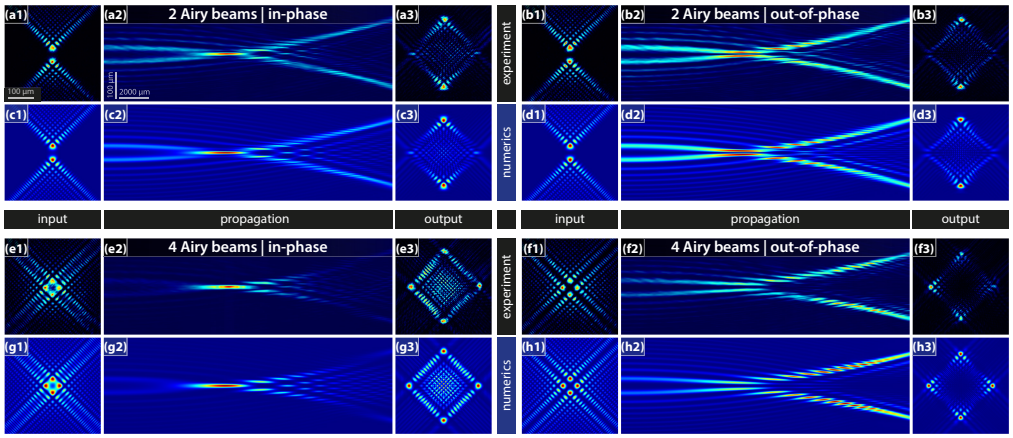


Fig. 2. Interference of multiple Airy beams in homogeneous linear medium. (a–d) Evolution of two Airy beams in experiment and numerics. (a,b) in phase, (c,d) with $\pi$ phase difference. (e–h) Evolution of four Airy beams in experiment and numerics. (e,f) in phase, (g,h) with $\pi$ phase difference. Each panel is normalized individually.

will intersect during propagation. The longitudinal position of this intersection point strongly depends on the curvature of the Airy beams which is determined by their size, but also depends on their initial separation. We aim to observe this defined intersection inside the volume of the 20 mm long SBN crystal. Therefore, we set the Airy beam size, measured as the distance between the main lobe and the next neighbor, to $s \approx 25\,\mu$m.

To visualize the complex evolution of the intensity distribution during propagation, we extract cross-sections through the experimentally recorded intensity volume along the coordinate in which the acceleration happens. Our experimental setup allows to retrieve this three-dimensional intensity volume by automatically recording the transverse intensity distribution in many (here 100) different planes along the crystal and stacking them. It is worth to mention that recording the intensity at planes inside the crystals is only possible if the refractive index between this plane and the camera is uniform, in other words, if the crystals in homogeneous.

The experimental results for two Airy beams are shown in Figs. 2(a) and 2(b), with the corresponding numerical simulations in Figs. 2(c) and 2(d). Thereby, we consider two cases where the beams are either in phase, or $\pi$ out of phase. These different initial conditions result in distinguishable transverse intensity profiles during propagation due to interference. For the in-phase configuration, depicted in Fig. 2(a) and 2(c), a well-pronounced focus is formed by constructive interference of the beams in the intersection region of both accelerated trajectories. This feature of a very high local intensity compared to the surrounding was previously emphasized as the key advantage of so-called autofocusing beams [32,33]. For the out-of-phase case, shown in Figs. 2(b) and 2(d), the phase difference of $\pi$ between the beams at the input leads to the vertical separation by a dark line of destructive interference which is preserved during the whole propagation. In both cases, the parabolic trajectories of the two superimposed Airy beams can clearly be identified. Since so far the propagation is completely linear, the complex intensity patterns results only from interference, but the beams do not interact and influence each other. Therefore, their initial general accelerated trajectories are preserved, albeit the beams trajectories intersect.

By increasing the number of the superimposed beams, the next symmetrical configuration can be constructed with four displaced Airy beams each rotated by 90°, as shown in Figs. 2(e)–2(h). In principle there are more possibilities to set the relative phases of the beams, but we

#246589 Received 23 Jul 2015; accepted 28 Jul 2015; published 8 Sep 2015

want to limit our studies to the following two cases: either all beams are in phase (Figs. 2(e) and 2(g)), or neighboring beams are $\pi$ out of phase (Figs. 2(f) and 2(h)). While the transverse intensity profiles now look quite different compared to the situation where two beams are superimposed, the longitudinal cross-sections reveal a similar propagation behavior. Again, a well-pronounced high-intensity focus is formed in the region where the four in-phase Airy beams interfere constructively, while the dark line of destructive interference always separates the beams in the out-of-phase case. Due to the fact that now four beams are interfering, the relative strength of the focus for constructive interference is much higher than for two beams. The number of interfering Airy beams could be further increased while the contrast between the focal intensity and the background continuously grows to the limit achieved by radially distributed Airy beams [32].

All presented experimental results are supported by corresponding numerical simulations. For the propagation of multiple Airy beams in the linear regime the numerical results perfectly fits to the experimental measurements. Although the wave equation (1) for homogenous media ($\Delta n(I) = 0$) has analytical solution in form of truncated Airy beams which can be explicitly calculated for any distance $z$, we already here employ the numerical beam propagation method to prove and emphasize that the simulation methods we developed precisely describe the real experimental conditions.

## 5. Nonlinear interaction of multiple two-dimensional Airy beams

From the above presented results we see, that during linear propagation of multiple Airy beams interference alone already leads to interesting intensity distributions, even as the beams do not interact and influence each other. If such an interdependency mediated by a nonlinear light matter interaction is included into the theoretical models and experiments, interesting novel effects can be expected, as for example soliton formation as predicted numerically in [26, 27].

In the following, we will investigate and analyze the nonlinear propagation and interaction of multiple Airy beams experimentally in photorefractive SBN. As introduced above, the refractive index of the nonlinear crystal depends non-locally on the incident intensity distribution and leads to a self-focusing, saturable nonlinearity. This complex nonlinearity completely changes the propagation dynamics of the Airy beams and leads to fascinating new types of beam evolution that depends amongst others on the number of superimposed beams, their relative phase and intensity. The experimental and numerical results for two and four superimposed Airy beams are presented in the following sections.

### *5.1. Interaction of two Airy beams*

We start our investigations about the nonlinear interaction with the most fundamental configuration of two displaced Airy beams. We use the same beam parameters as described above for the linear case (cf. Fig. 2). At the input, the two beams that are separated by $d \approx 50\,\mu\text{m}$ and are orientated to accelerate towards each other. Thereby, the trajectories of the undisturbed Airy beams would intersect and the beams strongly interact. In contrast to the linear experiment, we now increase the beam power, as well as the writing time to gain sufficient nonlinearity. To observe the intensity dependency of the propagation dynamics we set four different probe beam powers: $P_{\text{in}} \approx \{237,\ 475,\ 950,\ 1.425\}\,\text{nW}$ and perform the experiment for each value, while keeping all other parameters such as external field, induction time, and background illumination unchanged.

The experimental results for the in-phase beams are shown in Fig. 3(a). While increasing the probe beam power we can see the transition from the almost linear interference pattern Fig. 3(a1) to a well-localizes, solitary output state for higher nonlinearities Figs. 3(a3) and 3(a4). This localized state origins at the intersection point of the beam trajectories, where

#246589 Received 23 Jul 2015; accepted 28 Jul 2015; published 8 Sep 2015

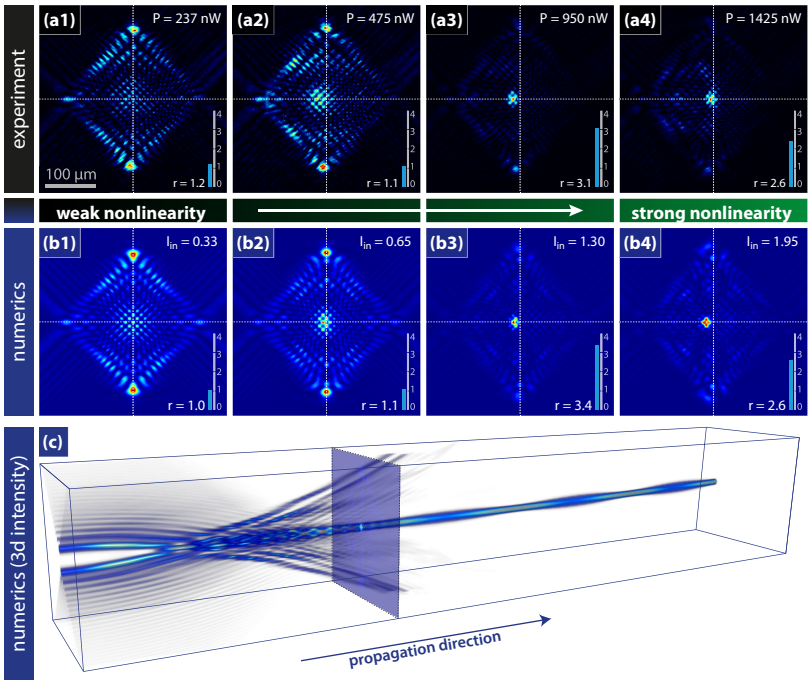


Fig. 3. Formation of solitary states from the interaction of two in-phase Airy beams. (a) Experimental results for different probe beam power. Each panel shows the intensity pattern at the output face of the SBN crystal (individually normalized). (b) Results from corresponding numerical simulations. (c) Volumetric plot of the numerically calculated three-dimensional intensity distribution (three times longer crystal) for strong nonlinearity. The position of the marked plane corresponds to the length of the used SBN crystal, $L = 20\,\mathrm{mm}$ and to Figs. (a4),(b4).

the constructive interference of the in-phase Airy beams leads to a strongly increased local intensity. Afterward, it propagates almost unchanged, except small breathing, due to the compensation of the diffraction by nonlinear self-focusing. The merged localized state further propagates straight obviously without any transverse momentum remaining from initial accelerated beams. The nonlinearity allows for this complex interaction between the two beams that in consequence compensates the acceleration. The peak intensity of the resulting state at the output of course is higher than the peak intensity at the input where the individual beams do not noticeably overlap. The factor $r = I_{\mathrm{max,out}}/I_{\mathrm{max,in}}$ (see insets in Fig. 3) represents the ratio between the maximal intensity at the output and the input, respectively. Due to the principal limitation that direct imaging through a non-homogeneous medium is not possible, only the output face of the SBN crystal is accessible for all nonlinear experiments throughout this paper. The factor $r$ helps to compare experiments and numerics also quantitatively.

The comparison between the experimental results Fig. 3(a) and the numerical simulation presented in Figs. 3(b) and 3(c) shows a very good overall agreement. According to the different probe beam powers in the experiment, we simulated the nonlinear propagation for different corresponding input intensities $I_{\mathrm{in}} \approx \{0.33, 0.65, 1.30, 1.95\}$. The output profiles, as well as the intensity factor $r$ perfectly matches the real observations in experiment. This verifies that our implemented numerical methods exactly describe the real situation and justify to employ numerical simulations to get a detailed impression what dynamics happens during nonlinear

#246589 Received 23 Jul 2015; accepted 28 Jul 2015; published 8 Sep 2015

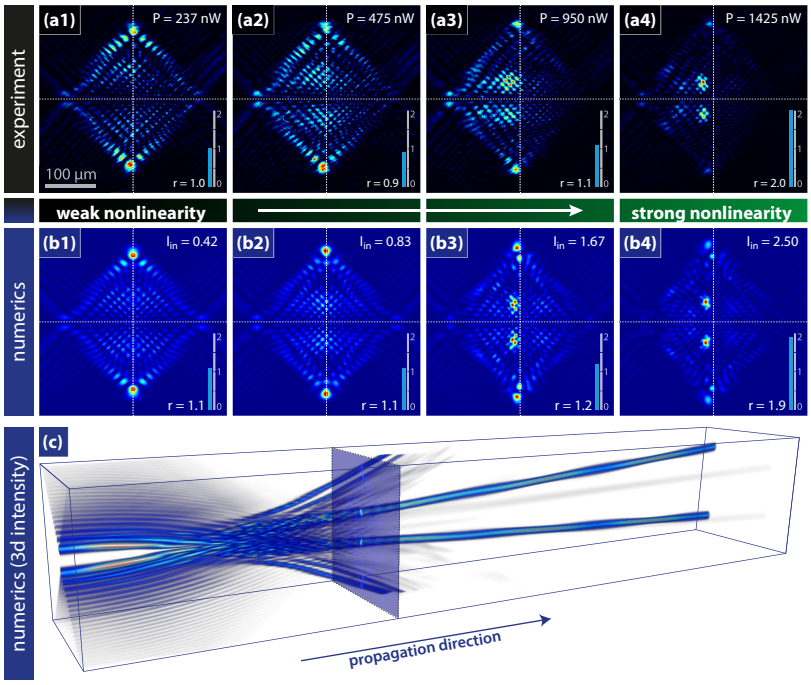


Fig. 4. Formation of solitary states from the interaction of two out-of-phase Airy beams. (a) Experimental results for different probe beam power. Each panel shows the intensity pattern at the output face of the SBN crystal (individually normalized). (b) Results from corresponding numerical simulations. (c) Volumetric plot of the numerically calculated three-dimensional intensity distribution (three times longer crystal) for strong nonlinearity. The position of the marked plane corresponds to the length of the used SBN crystal, $L = 20\,\mathrm{mm}$ and to Figs. (a4),(b4).

propagation in the SBN crystal. As mentioned above, in the experiment these data are not accessible due to principle physical reasons.

Figure 3(c) shows a volumetric rendering of the numerically retrieved intensity distribution during nonlinear propagation. The formation of the solitary state is clearly visible. While during the build-up process noticeable modulations in the shape and the intensity of the solitary state occurs (i.a. due to the passing of the remaining side lobes of the initial Airy beams), after some propagation distance the situation stabilizes and the solitary state propagates almost unchanged, except small breathing. The marked plane in Fig. 3(c) corresponds to the length of the SBN crystal and the pictures shown in Figs. 3(a) and 3(b).

A similar localization behavior was also found numerically for simpler idealized isotropic Kerr, and saturable Kerr nonlinearities [27]. For the presented experimental and numerical results in a realistic photorefractive SBN crystal, the situation is much more complicated, due to the anisotropic, saturable and drift-dominated nonlinearity. The slight shift of the intensity peaks in horizontal direction can be explained by additionally taking into account diffusion effects in the numerical model.

In the opposite case where the two Airy beams are $\pi$ out of phase, the situation is completely changed, as can be seen from the results shown in Fig. 4. The two main lobes do not merge (c.f. Figs. 2(b) and 2(d)) due to the separating line of destructive interference in the middle between the beams. As a consequence, two localized solitary spots build up and stably propagate as a

#246589 Received 23 Jul 2015; accepted 28 Jul 2015; published 8 Sep 2015

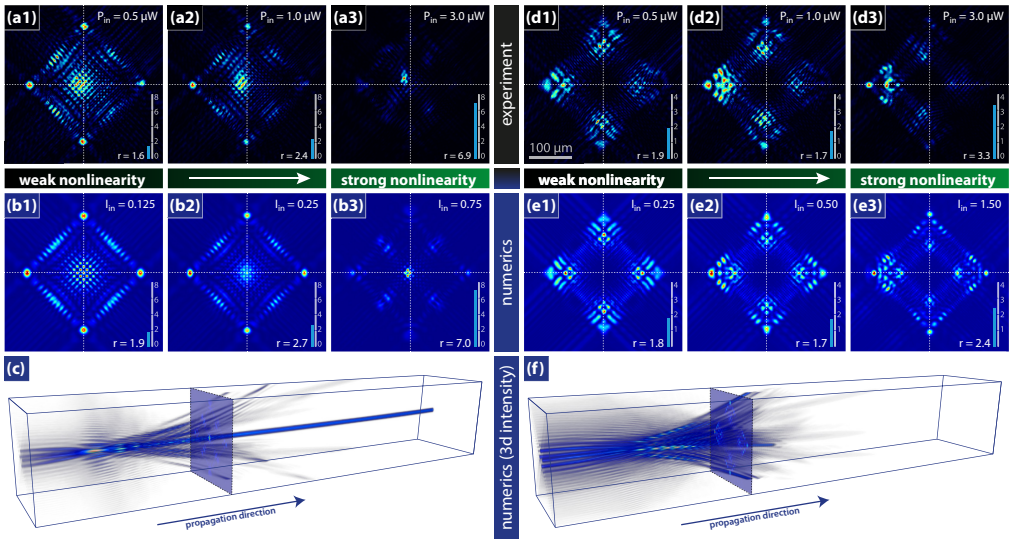


Fig. 5. Interaction of four Airy beams. (left) Formation of solitary state for the case where the beams are in phase. (right) Nonlinear propagation for $\pi$ phase difference. (a),(d) Experimental results for different probe beam power. Each panel shows the intensity pattern at the output face of the SBN crystal (individually normalized). (b,e) Results from corresponding numerical simulations. (c,f) Volumetric plot of the three-dimensional intensity distribution (from numerics) for strong nonlinearity.

pair over large distances. Again, the build-up process is accompanied by intensity modulations, but after a certain distance only small breathing remains. Introduced by the initial phase difference, these two solitons also have a phase difference of $\pi$ and hence repel each other, as reported for fundamental solitons [34]. Therefore, they propagate on straight lines but with a small divergence, as can bee seen in Fig. 4(c). The remaining side lobes of the initially launched Airy beams further follows their parabolic trajectory and quickly depart out of the volume.

### 5.2. *Interaction of four Airy beams*

After investigating the nonlinear processes for the fundamental case of two interacting Airy beams, we now turn towards the more advanced case where four beams are synthesized. The four Airy beams are combined in the way that their trajectories will intersect, as described above (c.f. Fig. 2). In general, four beams allow more than two different phase configuration with integer values in units of $\pi$, nevertheless we restrict ourselves to the two cases: either all beams are in phase, or with $\pi$ phase difference between neighboring beams. These two cases leads to completely different results.

For the case where all beam are in phase, the results are shown in Fig. 5 (left). Although the transverse intensity structure at the input face of the crystal looks different since now four beams are superimposed, the general nonlinear behavior is similar to the case where two Airy beams were launched in phase (c.f. Fig. 3). With increasing nonlinearity, the intensity localizes in the middle and forms a stable solitary state that emerges from the constructive interference of the beams in the region where their trajectories intersect. The experimental results for three different beam intensities $P_{\text{in}} \approx \{0.5, 1.0, 3.0\}\,\mu\text{W}$ (Fig. 5(a)) clearly show the described formation of the solitary state as the transition from the four separated Airy main lobes (see Fig. 5(a1)) to the high-intensity localized state (see Fig. 5(a3)). Here, the ratio $r$ between the maximal intensity at the input and the peak intensity of the built-up solitary state is much higher compared to

#246589 Received 23 Jul 2015; accepted 28 Jul 2015; published 8 Sep 2015

the two-beam case, which is understandable because four beams are merging.

The situation is completely changed for the configuration with a phase difference of $\pi$ between neighboring beams. The corresponding results are shown in Fig. 5 (right). In contrast to all other presented cases, here neither a straight soliton nor a soliton-pair or cluster is forming. Owed to the phase differences, no pronounced high-intensity spot arises from interference at the intersection of the beam trajectories that could develop into a soliton. Moreover, the remaining side lobes of the four Airy beams prevent the build-up of a solitary states or clusters, like it was observed in the previous case for two beams (Fig. 4). For higher intensities, the intensity tends to localize predominantly on one side (cf. Fig. 5(d3)) and keeps traveling away from the center.

Comparing all results of the nonlinear interaction of two and four Airy beams, we could identity three different types of nonlinear dynamic. First, in all cases where the synthesized beams are in phase, the interaction leads to the formation of one single stable spatial solitary state initiated by the high intensity resulting from constructive interference of the main lobes. The second type, the formation of a solitary pair, could be observed if two beams are superimposed with a phase difference of $\pi$. For these two types the acceleration of the initial Airy beams is exactly compensated, leading to straight propagating solutions. Interestingly, there is a third type where no solitary structures appears, even for the same intensities and nonlinearities. This could be observed if four Airy beams are superimposed with $\pi$ phase difference, as it was done in the last example. For this configuration the nonlinear dynamic shows symmetry-breaking behavior that depends critically on small perturbations and asymmetries in the system. The directed diffusion of charge carriers inside the photorefractive SBN crystals causes such an asymmetry, that is also responsible for the horizontal shift of the other solitary solutions, as reported above.

## Conclusion

In summary, we have presented the first experimental and numerical study about nonlinear interaction of multiple two-dimensional Airy beams. As the most important result, we could demonstrate the build-up of solitary structures from the nonlinear interaction of multiple accelerated beams. By investigating the nonlinear dynamic of the superimposed Airy beams for different configurations (numbers of beams, phase relations), we could demonstrate the intensity-dependent formation of straight propagating solitary states or pairs. These fundamental results could be achieved using a highly-developed experimental platform to perform nonlinear experiments which allows us to precisely shape the input beam as requested and reproducibly control all relevant parameters, such as input beam power, external electric field, and illumination time. Our experimental results and methods enable further investigations about the interaction of other types of tailored optical beams (e.g. nondiffracting beams) and moreover could find applications in modern optical information processing architectures as a basis for light guiding and switching approaches.

## Acknowledgments

This work is partially supported by the German Academic Exchange Service (Project 56267010) and Ministry of Education, Science and Technological Development, Republic of Serbia (Project OI 171036).

#246589 Received 23 Jul 2015; accepted 28 Jul 2015; published 8 Sep 2015